

Cite this: *J. Mater. Chem. C*, 2013, **1**, 5116

## When dithiafulvenyl functionalized $\pi$ -conjugated oligomers meet fullerenes and single-walled carbon nanotubes†

Karimulla Mulla and Yuming Zhao\*

A series of  $\pi$ -conjugated oligomers taking linear and Z-shaped molecular structures were synthesized with electron-donating dithiafulvenyl (DTF) groups functionalized at the terminal positions. Besides significantly enriched electronic and redox properties as disclosed by UV-Vis absorption and voltammetric analyses, these DTF-encapped oligomers also exhibited a facile reactivity of oxidative C=C bond cleavage sensitized by fullerenes under air, converting the non-fluorescent DTF-oligomers to highly fluorescent aldehyde-encapped oligomer products. This reaction provides an appealing approach for efficient fluorescence turn-on sensing of fullerenes. Furthermore, the DTF-attached oligomers showed strong noncovalent interactions with single-walled carbon nanotubes (SWNTs) to form soluble supramolecular assemblies in certain chlorinated organic solvents such as methylene chloride and chloroform. The dispersion of SWNTs effected by the DTF-oligomers was found to be highly efficient (up to 0.29 mg of SWNTs per mL) and shows selectivity for small-diameter nanotubes. The resulting SWNT suspensions could be easily dissociated upon addition of hydrocarbon solvents such as hexanes, releasing pristine SWNTs which were free of oligomer dispersants after filtration and solvent rinsing.

Received 4th April 2013

Accepted 14th June 2013

DOI: 10.1039/c3tc30626g

www.rsc.org/MaterialsC

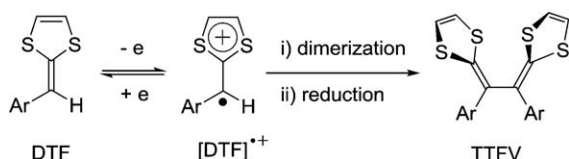
### Introduction

Dithiafulvene (DTF) acts as a good electron-donating group, since its dithiole ring, after releasing one electron, is converted into an aromaticity-stabilized dithiolium ion. Therefore, oxidation of an aryl-substituted DTF usually leads to a radical cation intermediate which swiftly undergoes a dimerization process, forming a new C–C bond and giving a tetrathiafulvene vinylogue (TTFV) product (Scheme 1).<sup>1</sup>

Because of its unique electrochemical reactivity, the DTF group has been used to functionalize various molecular structures, acting as a synthetic handle that enables further electrochemical coupling and/or polymerization to generate redox

active TTFV derivatives and related macromolecular systems.<sup>2</sup> The role of DTF in electronic substitution for structurally defined conjugated  $\pi$ -oligomer systems is still far from being thoroughly examined; nonetheless, there have been some studies in the recent literature which have addressed this topic. For instance, Roncali and co-workers made a class of star-shaped conjugated systems with a triphenylamine (TPA) core, and applied these molecular materials in polymer-based solar cells and electrochromism.<sup>3</sup> Garín and co-workers synthesized a series of donor–acceptor (D–A) functionalized oligoynes, where DTF was used as the electron donor to bring about enhanced second-order nonlinear optical (NLO) properties.<sup>4</sup> Very recently, Yang and co-workers reported that D–A endcapping of a diphenylthiophene  $\pi$ -framework using DTF as the electron donor could lead to remarkably increased device efficiency for dye-sensitized solar cells.<sup>5</sup> Our group has previously investigated a series of DTF-encapped oligoynes and disclosed their electronic properties as well as applicability in preparing electrochromic polymer films on conducting substrates *via* electropolymerization.<sup>6</sup>

In this contribution, we investigated the substitution effects of DTF on structurally defined  $\pi$ -conjugated oligomers. A group of oligo(phenylene ethynylene) (OPE) and oligo(phenylene vinylene) (OPV) based conjugated co-oligomers<sup>7</sup> were designed and synthesized in both the linear and Z-shaped structures for the study of structure–property relationships. Through a phosphite-promoted olefination reaction,<sup>8</sup> DTF endgroups were efficiently attached to the terminal positions of these oligomers, and the



Scheme 1 Oxidative dimerization of DTF.

Department of Chemistry, Memorial University, St. John's, NL, Canada A1B 3X7.  
E-mail: yuming@mun.ca; Fax: +1 709 863 3702; Tel: +1 709 864 8747

† Electronic supplementary information (ESI) available: Detailed spectroscopic, microscopic, and electrochemical characterization of new compounds and related SWNT dispersions. See DOI: 10.1039/c3tc30626g

resulting DTF-oligomer hybrids served as reasonable models to allow the interplay between DTF endgroups with the  $\pi$ -frameworks of conjugated oligomers to be compared and assessed. Our studies in this work have disclosed some unprecedented molecular and supramolecular behaviours arising from DTF functionalization. In particular, investigations on the photophysical properties of the DTF-oligomers have revealed an interesting C=C bond cleavage reaction promoted by singlet oxygen in the presence of fullerenes. This reaction converts non-fluorescent DTF-functionalized oligomers into highly fluorescent aldehyde-dependent oligomers, providing a new way for fluorescence turn-on sensing of fullerenes. On the other hand, the excellent electron donating property of DTF was also predicted to result in strong affinity for carbon-based nanomaterials. For example, Bao and co-workers recently reported the use of DTF/thiophene copolymers to disperse single-walled carbon nanotubes (SWNTs) for making thin film transistors.<sup>9</sup> In our work, supramolecular interactions between the DTF-oligomers and SWNTs have been examined. Although relatively small  $\pi$ -oligomers are not generally reckoned to induce sufficient dispersion of SWNTs in solution, to our great surprise, the DTF-functionalized oligomers not only gave rise to highly effective SWNT dispersion in certain organic solvents, but also enabled reversible control over the dispersion/releasing of SWNTs by a simple solvent effect. The following content describes the detailed synthesis of these DTF-oligomers and studies of their interesting molecular and supramolecular properties.

## Results and discussion

### Synthesis

Scheme 2 describes the synthetic routes to linear-shaped DTF-endcapped phenylacetylene oligomers. Sonogashira coupling of

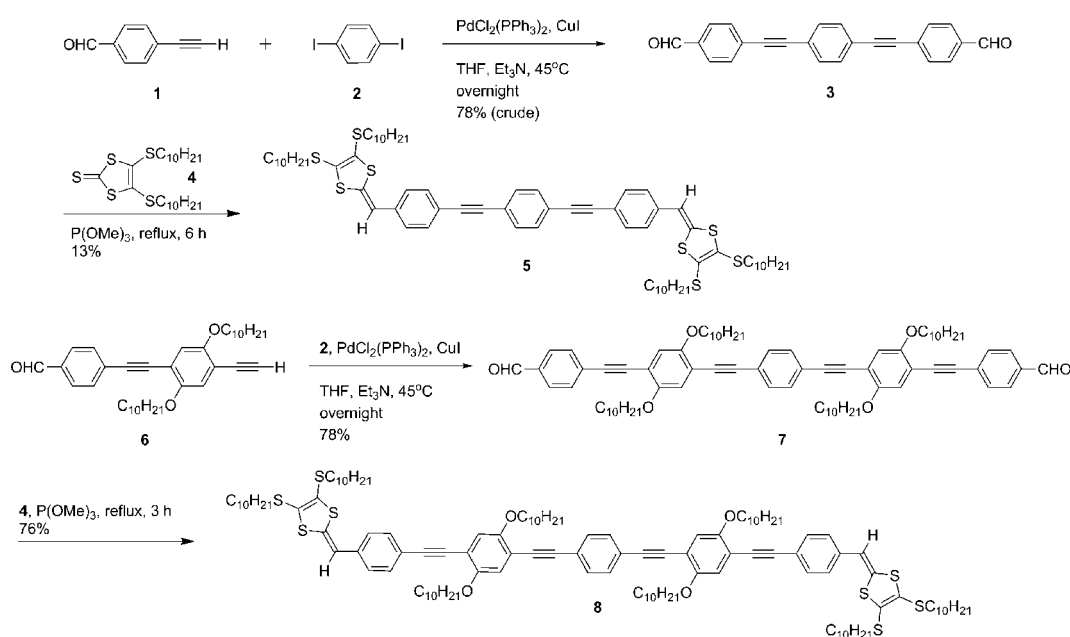
*p*-ethynylbenzaldehyde (**1**) with *p*-diiodobenzene (**2**) afforded oligomer **3** in a crude yield of 78%. Compound **3** showed very poor solubility in common organic solvents due to the lack of solubilizing groups, and was therefore obtained merely in a crude form. Despite the difficulty in attaining satisfactory purity, **3** was subjected to a P(OMe)<sub>3</sub>-mediated olefination reaction<sup>8</sup> with thione **4**,<sup>10</sup> giving DTF-endcapped phenylacetylene trimer **5** that showed much better solubility and was readily purified by column chromatography. Through an approach similar to the synthesis of **5**, a longer OPE framework **7** was prepared from Sonogashira coupling of compound **6** with *p*-diiodobenzene (**2**). The aldehyde groups of **7** were then subjected to an olefination reaction, furnishing DTF-endcapped phenylacetylene pentamer **8** in a good yield of 76%.

The construction of Z-shaped OPE/OPV co-oligomers is outlined in Scheme 3. First, a Wittig-Horner reaction<sup>7b,c</sup> was performed between *o*-iodobenzaldehyde (**9**) and bisphosphonate **10** in the presence of NaH to give diiodo-OPV **11** in 46% yield. Compound **11** underwent a double Sonogashira coupling with compound **1** to yield Z-shaped oligomer **12**, which was then converted into DTF-OPE/OPV **13** through the P(OMe)<sub>3</sub>-promoted olefination.<sup>8</sup> By a similar sequence of Sonogashira coupling and olefination, a longer Z-shaped DTF-OPE/OPV **15** was produced in a very good yield.

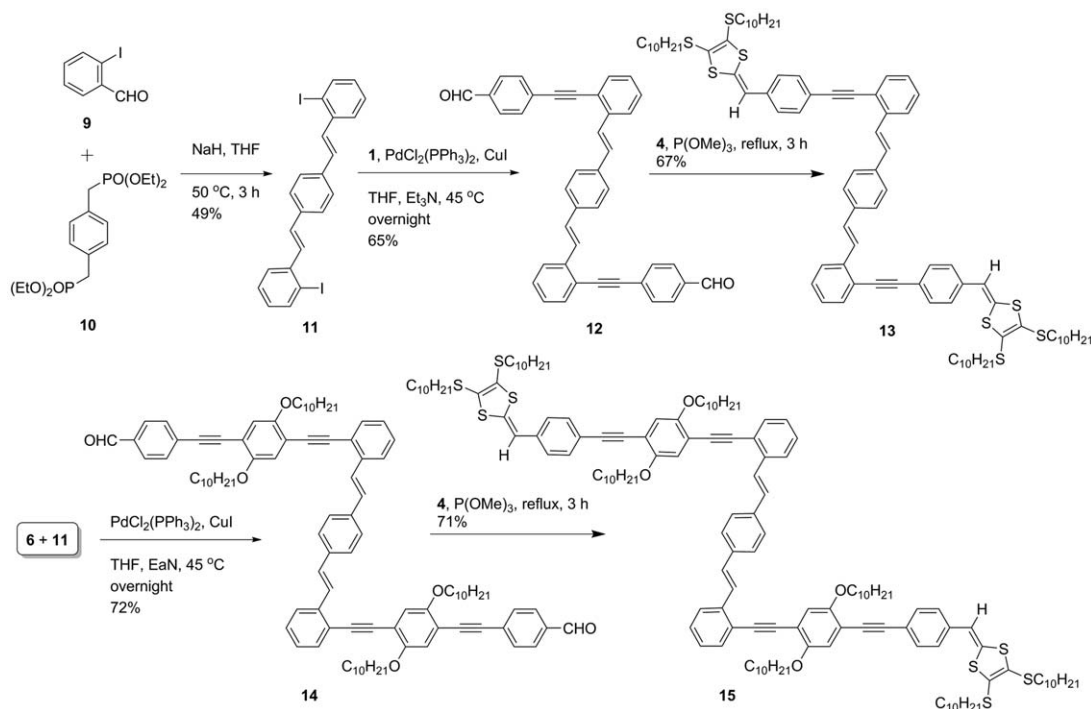
### Electronic absorption and emission properties

Fig. 1 shows the UV-Vis absorption spectra of DTF-oligomers in comparison with their aldehyde-oligomer precursors except compound **3** due to its limited solubility. The detailed absorption spectroscopic data are summarized in Table 1.

It can be seen from Fig. 1A that the maximum absorption wavelength of long linear DTF-OPE **8** (at 423 nm) is redshifted by only 12 nm relative to short DTF-OPE **5** (at 412 nm), as a



**Scheme 2** Synthesis of linear OPEs with DTF endgroups.



**Scheme 3** Synthesis of Z-shaped OPE/OPV co-oligomers with DTF endgroups.

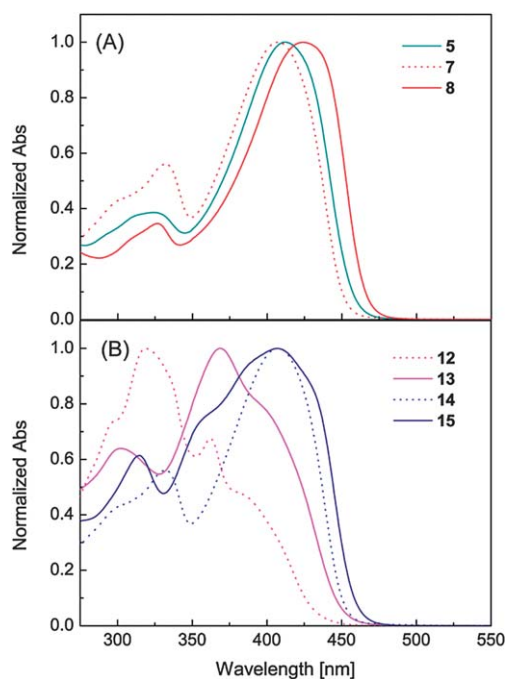


**Fig. 1** Normalized UV-Vis absorption spectra of oligomers **5**, **7**, **8**, and **12–15** measured in  $\text{CHCl}_3$  at room temperature.

consequence of an increased  $\pi$ -conjugation degree of the oligomer framework. Comparison of the absorption spectra of DTF-OPE **8** and aldehyde-OPE **7** ( $\lambda_{\text{max}} = 408 \text{ nm}$ ) reveals a redshift of  $\lambda_{\text{max}}$  by 15 nm, which is ascribed to the substitution effect of DTF endgroups on the electronic properties of the

**Table 1** Summary of photophysical data for DTF-oligomers and their aldehyde-oligomer precursors

Entry	Absorption $\lambda/\text{nm}$ ( $\epsilon/10^4 \text{ cm}^{-1} \text{ M}^{-1}$ )	Emission <sup>a</sup> $\lambda/\text{nm}$	Quantum yield ( $\Phi$ )
<b>5</b>	412 (6.72), 319 (2.56)	488, 466	0.012
<b>7</b>	407 (7.92), 331 (4.45), 299 (3.42),	485, 454	0.591
<b>8</b>	423 (11.2), 326 (3.82)	487, 468	0.0134
<b>12</b>	387 (2.51), 361 (3.65), 318 (5.38)	487, 462	0.406
<b>13</b>	296 (3.98), 246 (1.78), 402(s) (4.90), 368 (6.49), 301 (4.14)	444	0.0109
<b>14</b>	401(s) (6.21), 366 (7.65), 327 (5.98), 308 (6.41)	487, 474	0.676
<b>15</b>	432 (8.47), 406 (10.5), 384 (9.33), 357 (7.52), 314 (6.19), 245 (5.04)	488, 466	0.0131

<sup>a</sup> For **13** and **14**, excitation wavelength ( $\lambda_{\text{ex}}$ ) = 350 nm; for **5**, **7**, **8**, **12** and **15**,  $\lambda_{\text{ex}}$  = 370 nm.

oligomer unit. The spectrum of short Z-shaped DTF-OPE/OPV **13** shows a low-energy absorption band at 368 nm along with a shoulder at 402 nm. Its aldehyde precursor **12** exhibits a similar low-energy spectral profile, but the absorption band and shoulder are slightly blueshifted to 361 nm and 387 nm respectively. The spectrum of long Z-shaped DTF-OPE/OPV **15** shows a maximum absorption band at 408 nm, which is similar to that of its aldehyde precursor **14** ( $\lambda_{\text{max}} = 407 \text{ nm}$ ). The spectrum of **15** shows a distinctive absorption band at 388 nm and a shoulder at 432 nm in the low-energy region.

The electronic emission properties of DTF-functionalized OPEs and related aldehyde-oligomer precursors were investigated by fluorescence spectroscopic analysis. The aldehyde-encapped oligomers are highly fluorescent (Fig. 2A) with quantum yields in the range of *ca.* 40–70% (see Table 1). For the DTF-encapped oligomers, however, the emission is substantially attenuated with quantum yields around *ca.* 1% (see Table 1). The reduced emission can be explained by a non-radiative decay mechanism in which photoinduced electron transfer (PeT) from a DTF donor to the oligomer fluorophores competes effectively with fluorescent emission.

### Electrochemical properties

The electrochemical redox properties of DTF-functionalized oligomers were investigated by cyclic voltammetry (CV). Fig. 3 shows the cyclic voltammograms that were measured in the multi-cycle scan mode.

In the first cycle of CV scans, the voltammogram of DTF-OPE 5 clearly shows an anodic peak at +0.82 V and a cathodic peak at +0.54 V, which are assigned to the oxidation of DTF into  $[DTF]^+$  and reverse reduction.<sup>1,6</sup> Starting from the second cycle of CV scans, a new anodic peak at *ca.* +0.6 V emerges and its intensity grows steadily with the increasing cathodic peak at +0.54 V. The rise of this new peak is due to the continuous formation of  $[TTFV]^{2+}$  as a result of oxidative dimerization of DTF (see Scheme 1) on the surface of the working electrode.<sup>1,6</sup> The voltammogram of longer DTF-OPE 8 shows a similar growth of the  $[TTFV]^{2+}$  peak upon multi-cycle scans; however, the  $[DTF]^+$  peak at *ca.* +0.82 V appears to reduce more dramatically in intensity in comparison with 5. Rationalization for the different CV

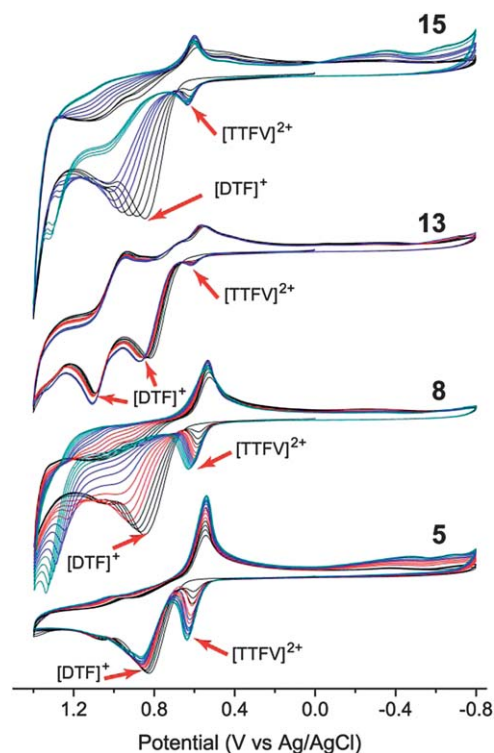


**Fig. 3** Cyclic voltammograms of DTF-oligomers measured in the multi-cycle scan mode. Experimental conditions:  $Bu_4NBF_4$  (0.1 M) as the supporting electrolyte,  $CH_2Cl_2$  as the solvent, glassy carbon as the working electrode, Pt wire as the counter electrode, Ag/AgCl as the reference electrode, and scan rate =  $100\text{ mV s}^{-1}$ .

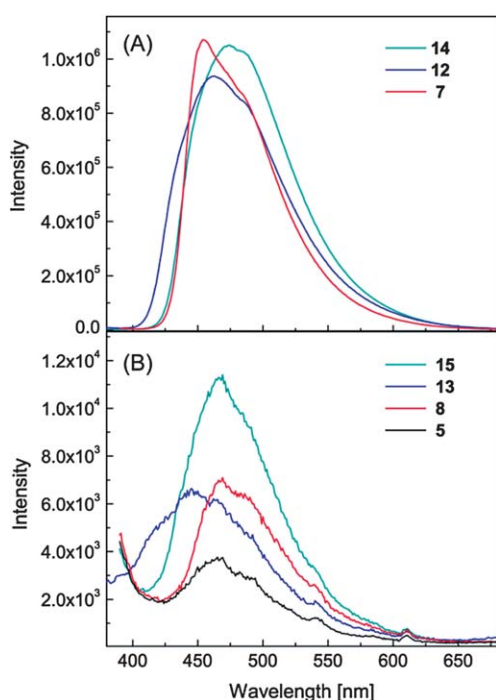


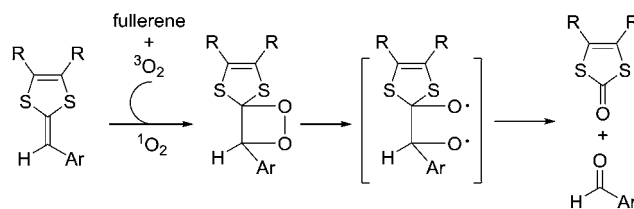
**Fig. 2** Fluorescence spectra of oligomers 5, 7, 8, and 12–15 measured in  $CHCl_3$  at room temperature.

patterns can be made as follows: when one of the DTF groups in 5 undergoes oxidative dimerization, the resulting  $[TTFV]^{2+}$  dication imposes a significant electron-withdrawing effect on the other DTF group *via* the relatively short OPE  $\pi$ -spacer, which in turn lowers its reactivity toward further oxidative dimerization. The electrochemical reactions on the working electrode therefore are mainly dimerization or low-degree oligomerization of 5, after which a significant amount of DTF endgroups still remain intact. For DTF-OPE 8, however, the relatively longer OPE bridge attenuates electronic communications between the two DTF endgroups. As a result, each of them undergoes oxidative dimerization independently, resulting in a quicker consumption of DTF units and relatively higher degree of polymerization upon multiple CV scans. The voltammogram of long Z-shaped DTF-OPE/OPV 15 shows similar electrochemical behavior to that of long linear DTF-OPE 8. Of particular note are the CV features of short Z-shaped DTF-oligomer 13. In the first cycle of scans, two anodic peaks at +0.82 V and +1.09 V and two cathodic peaks at +0.56 V and +0.94 V can be seen. This result suggests that the two DTF groups in 13 have a significant degree of electronic communications such that they are oxidized in a stepwise rather than a simultaneous manner. As the cycles of CV scans increase, the  $[TTFV]^{2+}$  peak at *ca.* +0.61 V becomes observable but with a very weak current intensity. The voltammogram of 13 clearly shows that its DTF endgroups are relatively unreactive towards oxidative dimerization. Such different electrochemical behaviour is attributable to the strong

electronic communications between the two DTF groups *via* the short Z-shaped OPE/OPV  $\pi$ -bridge of **13**. Overall, our comparative CV analyses confirm that the  $\pi$ -spacers have a key effect on the electrochemical reactivities of DTF-encapped oligomers.

### Fullerene-sensitized photo-oxygenation of DTF-oligomers and consequential fluorescence sensing for fullerenes

When a small amount of fullerene ( $C_{60}$  or  $C_{70}$ ) was added into the diluted solutions of DTF-oligomers, steadily increased fluorescence was observed. This property at the first look was a bit puzzling, given the known fluorescence quenching effects arising from both DTF endgroups and fullerenes on oligomer fluorophores. To shed light on this issue,  $^1H$  NMR analysis was performed on a mixture of oligomer **15** and  $C_{60}$  fullerene in deuterated benzene ( $C_6D_6$ ) at various time intervals, with the solution not being deliberately degassed. The NMR spectra shown in Fig. 4 unambiguously delineate a process in which the DTF units of oligomer **15** are gradually converted into aldehyde groups, leading to compound **14** and thione as the products. In addition to the NMR test, the reaction has also been attempted on a larger scale, where **15** (*ca.* 10 mg) was converted into **14** in a high yield of 89% (isolated) in the presence of  $C_{60}$  (3 molar equiv.) at room temperature within 20 hours. Fullerene  $C_{60}$  has a wide spectral absorption range and a low-lying triplet state.<sup>11</sup> It is therefore reasonable to assume that upon exposure to ambient light, a fullerene-sensitized reaction pathway leads to singlet oxygen ( $^1O_2$ ) formation.<sup>12</sup> Singlet oxygen is known to react with electron-rich alkene to form 1,2-dioxetane, which subsequently undergo O–O bond breaking to yield C=O products.<sup>13</sup> Scheme 4 shows a proposed mechanism accounting for the transformation of DTF to aldehyde induced by singlet oxygen. Non-fluorescent DTF-oligomers undergoing this singlet oxygen involved C=C cleavage reaction hence afford highly



**Scheme 4** Proposed mechanism for singlet oxygen-induced C=C bond cleavage of DTF.

fluorescence aldehyde-oligomers, giving rise to the observed fluorescence enhancement. The involvement of singlet oxygen as an oxidant in the fullerene-sensitized C=C bond cleavage is evidenced by the following experimental observations: (i) the reaction rate was considerably slowed down when the reaction was carried out under argon. (ii) The use of a classical singlet oxygen sensitizer, methylene blue, in place of  $C_{60}$ , also led to the same C=C bond cleavage reaction. (iii) Upon UV light irradiation under air, a condition known to generate singlet oxygen, compound **15** underwent the same C=C bond cleavage reaction as well without the presence of  $C_{60}$  (see ESI for detailed experimental results†).

To further probe the kinetic properties of the fullerene-sensitized C=C bond photo-oxygenation and subsequent cleavage reactions, diluted solutions of **15** mixed with either  $C_{60}$  or  $C_{70}$  fullerene were examined by fluorescence spectroscopic analysis at varied times (Fig. 5). From Fig. 5A, the fluorescence enhancement ( $F - F_0$ ) is observed to show a linear relationship with reaction time ( $\tau$ ) in the first 16 hours. Assuming that ( $F - F_0$ ) is proportional to the concentration of fluorescent product **14**, the correlation is in line with zero-order kinetics. When  $C_{70}$  was used *in lieu* of  $C_{60}$  as the

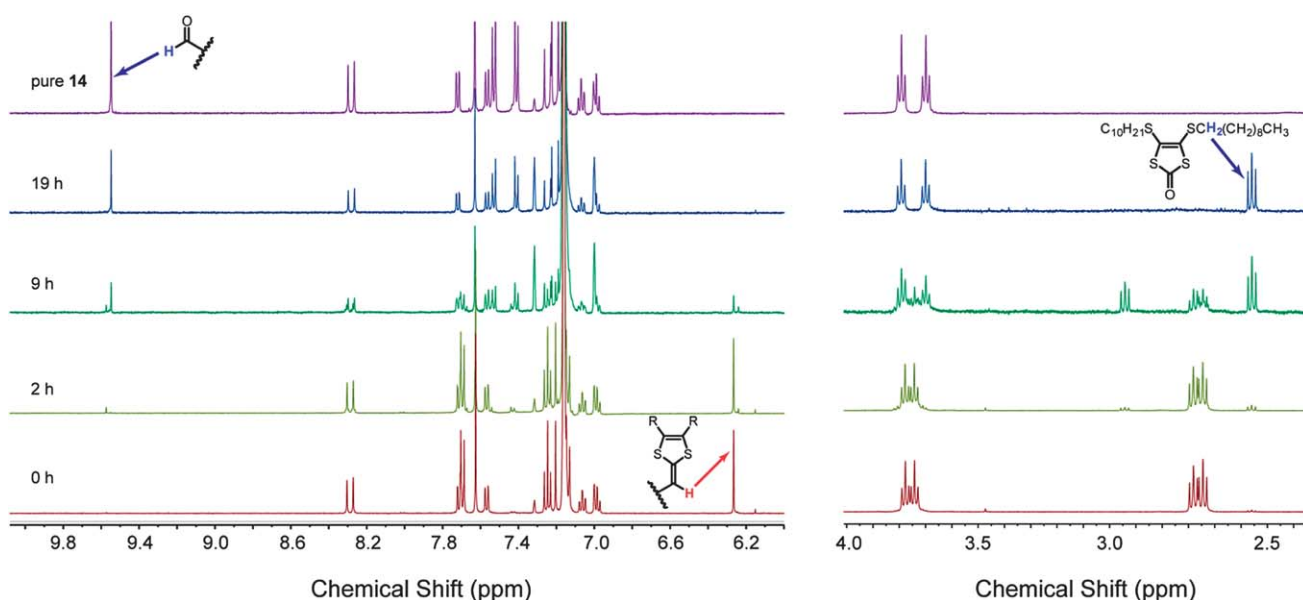


**Fig. 4**  $^1H$  NMR spectra in the aromatic and aliphatic regions showing the gradual conversion of DTF-oligomer **15** to aldehyde-oligomer **14** in the presence of  $C_{60}$  fullerene at 298 K. Initial concentration of **15**:  $8.9 \times 10^{-4}$  M, concentration of  $C_{60}$ :  $26.7 \times 10^{-4}$  M, and solvent:  $C_6D_6$ .

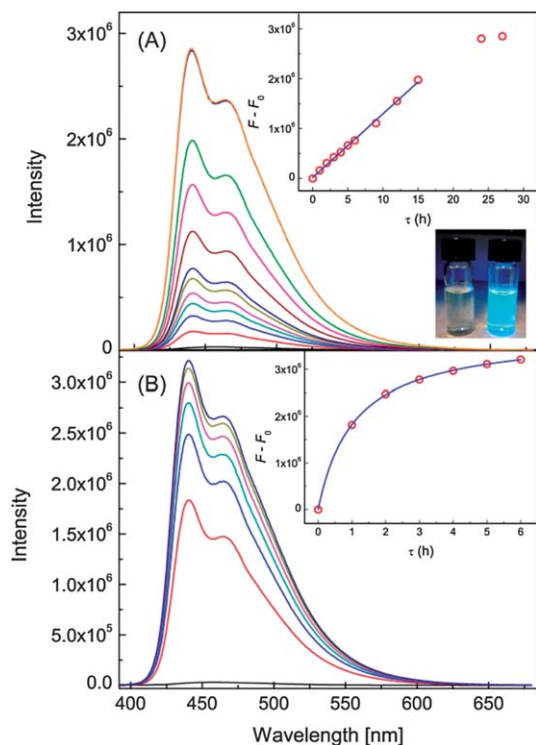
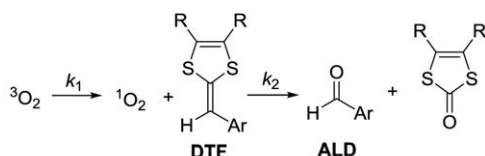


**Fig. 5** (A) Fluorescence spectra of **15** ( $1.8 \times 10^{-6}$  M) with  $C_{60}$  in benzene at varied times. (B) Fluorescence spectra of **15** with  $C_{70}$  in benzene at varied times. Inset plots: fluorescence enhancement ( $F - F_0$ ) as a function of time ( $\tau$ ).  $F_0$  and  $F$  denote fluorescence intensities measured at initial and later stages at 440 nm. Inset image: a photograph of **15** mixed with  $C_{60}$  in benzene taken at 0 h (left) and 24 h (right) under UV light irradiation.

sensitizer, the correlation of ( $F - F_0$ ) with  $\tau$  appears to be in a good agreement with a first-order kinetics. A tentative rationalization on these different kinetic properties can be made based on the kinetic analysis described in Scheme 5. In the case where singlet oxygen generation is the rate determining step and the concentration of dissolved oxygen in solution is deemed as constant, a steady-state approximation can be made to give zero-order behaviour for the observed reaction rate. In contrast, if the C=C bond cleavage is the rate determining step, a rapid equilibrium approximation is valid, which leads to a first-order kinetics for the overall reaction. The results of kinetics analysis suggest that  $C_{70}$  produces singlet oxygen at a much faster rate than  $C_{60}$ . A systematic survey on the kinetic



if  $k_1 \ll k_2$ , and  $[^3\text{O}_2] = \text{constant} \Rightarrow \text{Rate} = k_1[^3\text{O}_2]$ , zero-order

if  $k_1 \gg k_2$ , and  $[^1\text{O}_2] = \text{constant} \Rightarrow \text{Rate} = k_2[^1\text{O}_2][\text{DTF}]$ , first-order

**Scheme 5** Kinetics of singlet oxygen induced C=C bond cleavage of aryl-DTF.

properties is currently underway and the results will be disclosed in due course. It is worth noting that the fullerene-sensitized photo-oxygenation reaction of **15** at the DTF moiety gives a substantial increase in the fluorescence efficiency of the DTF-oligomer solution. For instance, the solution of **15** in benzene was found to show a substantial fluorescence enhancement of 149-fold after mixing with  $C_{60}$  fullerene for 24 hours, and 162-fold with  $C_{70}$  for 6 hours. The dramatic fluorescence response to fullerenes can be useful for further developing highly efficient detection methods and quantification protocols for different types of fullerenes.

### Supramolecular interactions of DTF-oligomers with SWNTs

Noncovalent functionalization of SWNTs has received considerable attention in the field of nanotube-based science and technologies, not only because it provides a direct solution to the problems of insolubility and poor processability of as-produced SWNTs, but also because it enables easy ways for sorting specific types of SWNTs out of as-produced SWNT mixtures.<sup>14</sup> Usually, macromolecule-based dispersants such as surfactants, polymers, and DNA are preferred for debundling and dispersion of SWNTs in various solvents, as they tend to form stable complexes with SWNTs with sufficient dispersant-SWNT interactions *via* van der Waals forces or  $\pi$ -stacking. The use of relatively small  $\pi$ -conjugated oligomers to disperse SWNTs, however, has not been extensively studied yet. In recent years, various DTF- and TTF-containing compounds have been found to show significant supramolecular interactions with SWNTs.<sup>9,15</sup> These results thus inspired us to investigate the supramolecular interactions between the DTF-oligomers and the SWNTs. In this work, two commercially available SWNT products, namely HiPCO and CoMoCAT nanotubes, were chosen for study. The dispersion experiments were conducted in a straightforward manner: a suitable amount of SWNT sample was added to the solution of a DTF-oligomer (*ca.*  $10^{-3}$  M<sup>-1</sup>) in a selected solvent. The mixture was ultrasonicated for 1 hour at room temperature and then subjected to a sequence of filtration, centrifugation, and filtration treatments. The filtrate solution was let stand still for a few hours and then checked both visually and by UV-Vis-NIR analysis. The photographic images in Fig. 6 depict the outcomes of HiPCO SWNTs dispersed with DTF-oligomers, from which it is clearly seen that HiPCO SWNTs form stable black suspensions in the chloroform solutions of all four DTF-oligomers, where long oligomers **8** and **15** give much better dispersion results than short oligomers **5** and **13**. In methylene chloride, long oligomers **8** and **15** can also induce efficient dispersion of HiPCO SWNTs, but short oligomers **5** and **13** cannot. For other common organic solvents, including chlorobenzene, toluene, and hexanes, no effective dispersion of HiPCO SWNTs can be obtained using DTF-oligomers as dispersants. Although both short and long Z-shaped oligomers **13** and **15** were able to effect dispersion of SWNTs in chlorobenzene immediately after sonication and filtration through a cotton plug, the suspensions were not stable enough and SWNTs precipitated out of the solution within a short period of time.

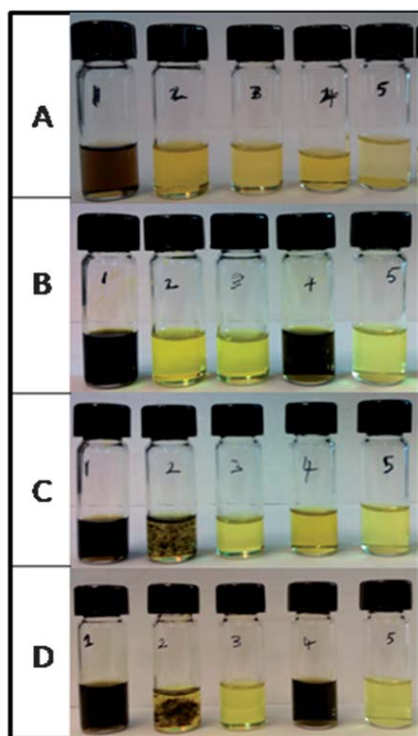


**Fig. 6** Photographic images of filtrates of DTF-oligomer solutions mixed with HiPCO SWNTs after sonication for 1 h. Rows: (A) oligomer **5**, (B) oligomer **8**, (C) oligomer **13**, and (D) oligomer **15**. Solvents tested (from left to right): chloroform, chlorobenzene, toluene, methylene chloride, and hexanes.

The solvent effect on dispersion turns out to be valuable for processing SWNTs, since it allows reversible releasing of SWNTs to be readily accomplished by a simple solvent mixing control. For instance, when an equal amount of hexanes was added to the stable suspension of HiPCO SWNTs and oligomer **15** in chloroform, SWNTs immediately precipitated out of the solution (see Fig. 7), and they were readily separated by vacuum filtration. The filtrate solution was then checked by UV-Vis-NIR analysis, showing that only a trace amount of SWNTs remained in the solution phase after this treatment. By this way, pristine SWNTs were conveniently recovered from the dispersion. The actual solubility of SWNTs in DTF-oligomer solutions was then determined. As listed in Table 2, the solubility of SWNTs in the

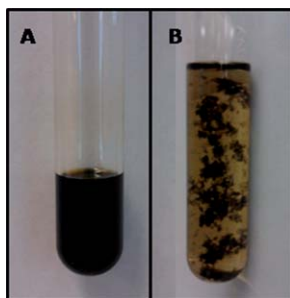


**Fig. 7** Photographic images of (A) HiPCO SWNT suspension with **15** in chloroform and (B) after addition of an equal amount of hexanes.

solutions of long oligomers **8** and **15** is much greater than in short oligomers **5** and **13**, likely due to their longer  $\pi$ -conjugated lengths and more solubilizing decyl side chains.

The HiPCO SWNTs released from the suspension in the solution of **15** were examined by Raman spectroscopy. As shown in Fig. 8, the spectrum of the released SWNTs shows only one significant peak at  $272\text{ cm}^{-1}$  in the region of radial breathing mode (RBM). The spectral feature is quite similar to that of the HiPCO SWNTs dispersed in the chloroform solution of **15**. For pristine SWNTs, the Raman spectrum shows two significant peaks at 267 and 225 nm respectively. Given the fact that the Raman frequency in this region is inversely proportional to the diameter of the nanotubes,<sup>16</sup> it is concluded that oligomer **15** can selectively disperse the nanotubes of relatively smaller diameters in pristine HiPCO SWNTs. The dispersion and releasing behaviours combined together offer a simple and effective method for sorting the small-diameter species out of the as-produced HiPCO SWNTs. Reversible dispersion and release of SWNTs using stimuli-responsive dispersants have received growing attention in recent years.<sup>17</sup> It is important to note that the released SWNTs are cleanly separated from oligomer dispersants, which is evidenced by Raman spectroscopic analysis. As shown in Fig. 9, the spectrum of the released SWNTs does not show significant signals at *ca.*  $2200\text{ cm}^{-1}$ , which is due to the  $\text{C}\equiv\text{C}$  stretching mode of oligomer **15**. In the fabrication of SWNT-based semiconducting electronic devices, suitable noncovalent pre-treatment of SWNTs such as selective dispersion is usually conducted. However, it is known that

**Table 2** Solubility of HiPCO SWNTs in DTF-oligomer chloroform solutions

Entry	Concentration of oligomer (mM)	Solubility of SWNTs (mg mL <sup>-1</sup> )
<b>5</b>	2.34	0.01
<b>8</b>	1.58	0.20
<b>13</b>	2.00	0.05
<b>15</b>	1.39	0.29

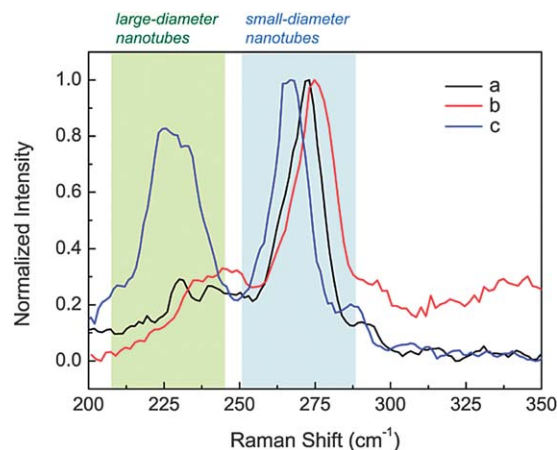


**Fig. 8** Normalized Raman spectra showing the RBM region of (a) HiPCO SWNTs released from the dispersion, (b) HiPCO SWNTs dispersed with **15**, and (c) pristine HiPCO SWNTs.

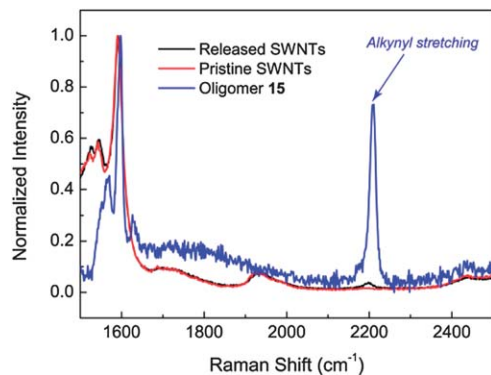


**Fig. 9** Normalized Raman spectra of the released SWNTs, pristine SWNTs, and pure oligomer **15** in the region of 1500 to 2500  $\text{cm}^{-1}$ .

organic dispersants introduced in the dispersion process tend to cause negative effects on the semiconducting properties of SWNTs, which in turn significantly reduce the device performance. To avoid this trouble, the interactions between dispersants and SWNTs are desired to be reversible. The solvent-controlled reversibility observed in the interactions between the DTF-oligomers and the HiPCO SWNTs thus contribute a useful method for this application.

The HiPCO SWNTs dispersed by DTF-oligomers **5**, **8**, **13**, and **15** in chloroform were further investigated by UV-Vis-NIR and Raman spectroscopic analysis. As can be seen from Fig. 10, the Vis-NIR absorption and Raman spectral profiles of the SWNTs dispersed by the four oligomers are very similar to one another. Since these analytical data are directly correlated with the structures and electronic types of SWNTs, the outcome indicates that the four DTF-oligomers show a similar selectivity for the types of nanotubes to be dispersed.

The microscopic properties of HiPCO SWNTs dispersed with DTF-oligomers were examined by atomic force microscopic (AFM) analysis. The AFM studies have revealed significant interactions between individual strands of SWNTs and the DTF-oligomers. For example, Fig. 11 shows the morphology of HiPCO SWNTs dispersed with long linear-shaped DTF-oligomer **8**, wherein oligomer agglomerates are clearly observed to stack around the sidewalls of debundled SWNTs. Such interactions are believed to be the major driving force for effective dispersion of SWNTs in the solution phase.

At this juncture, there are several points worth remarking: (1) the dispersion of HiPCO SWNTs with DTF-oligomers appears to be particularly effective in chloroform. The exact reason is unclear and awaits further investigation. Nevertheless,  $^1\text{H}$  NMR analysis on DTF-oligomer **15** discloses a dramatic degree of changes in the resonance frequencies of aromatic protons in different solvents (see Fig. S20, ESI†). Of particular note is that one of the vinyl protons was found greatly downfield shifted from 7.84 ppm (in  $\text{CDCl}_3$ ) to 8.29 ppm (in  $\text{C}_6\text{D}_6$ ). This behaviour is indicative of substantial changes in conformation and aggregation states in different solvent systems,<sup>18</sup> which is believed to cause the different dispersion outcomes in various solvents. Nonpolar chlorinated solvents such as chloroform and methylene chloride happen to solubilize the supramolecular

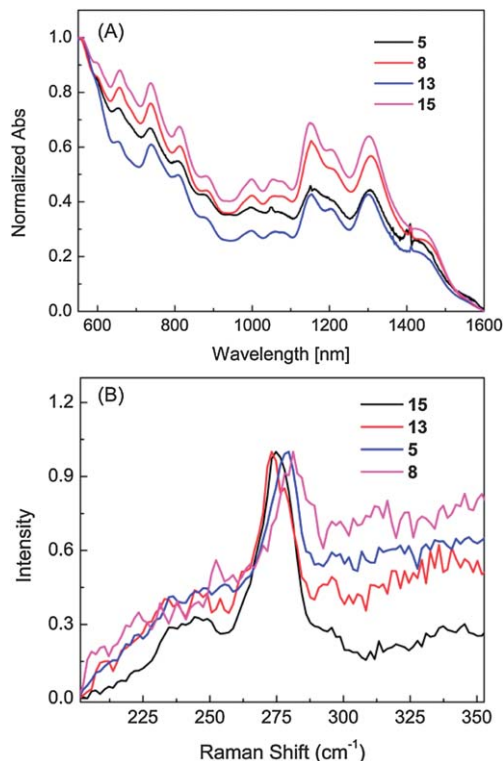


**Fig. 10** (A) Normalized UV-Vis-NIR spectra of HiPCO SWNTs dispersed by DTF-oligomers in chloroform. (B) Raman spectra of HiPCO SWNTs dispersed by DTF-oligomers in the RBM region ( $\lambda_{\text{ex}} = 534 \text{ nm}$ ).

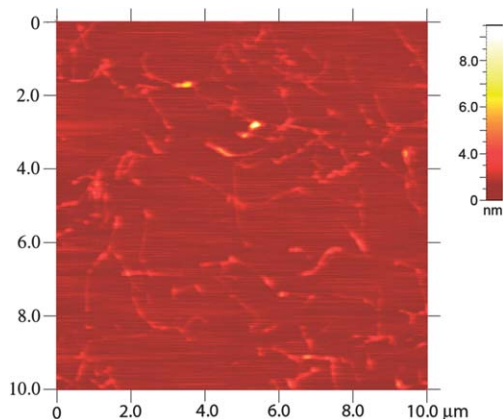


**Fig. 11** AFM image of supramolecular assemblies of HiPCO SWNTs and oligomer **8** spin-cast on a mica surface (tapping mode).

assemblies of DTF-oligomers and HiPCO SWNTs more effectively than other organic solvents. (2) The pristine SWNTs can be easily released from the oligomer-SWNT assemblies dispersed in chloroform by addition of another organic solvent such as hexanes to it. (3) The dispersion of CoMoCAT SWNTs by the DTF-oligomers appears to be less effective than HiPCO SWNTs. In fact, only the long linear oligomer **8** was found to induce a modest degree of dispersion in chloroform as evidenced by UV-Vis-NIR analysis (see Fig. S28, ESI†). This observation suggests that the interactions between DTF-oligomers

and SWNTs are dependent on the types of nanotubes. (4) The DTF group is a crucial and indispensable factor to SWNT dispersion. This point has been confirmed by a comparative study in which the aldehyde-oligomer precursors (3, 7, 12, and 14) were tested for SWNT dispersion under the same conditions used by the DTF-oligomers. The results clearly showed that, without DTF groups, the  $\pi$ -oligomers could not induce any effective dispersion on SWNTs in common organic solvents.

## Conclusions

In summary, we have synthesized a series of DTF-encapped OPE/OPV hybrid conjugated oligomers in a linear and Z-shaped molecular structure. The electronic and electrochemical properties of the DTF groups have been found to vary with the properties of the  $\pi$ -oligomer. As a strong electron donor, the DTF group exerted a substantial quenching effect on the fluorescence emission of the  $\pi$ -oligomers. When the DTF-encapped oligomers were mixed with fullerenes (C<sub>60</sub> and C<sub>70</sub>), the C=C bond of DTF would undergo a facile oxidative cleavage reaction under air and ambient light to form highly fluorescent aldehyde-encapped oligomers as the product. A fullerene-sensitized photooxygenation mechanism has been proposed to rationalize this reaction, while C<sub>70</sub> fullerene appeared to be a more efficient sensitizer than C<sub>60</sub> in promoting this unique reaction. The consequence of this reaction is a substantial fluorescence turn-on response to fullerenes by these DTF-oligomers, suggesting potential use in fullerene sensing and recognition. The DTF endgroups have imparted the  $\pi$ -oligomers with remarkable effectiveness at dispersing SWNTs in chloroform or methylene chloride. The dispersion outcomes are highly solvent-dependent and very easy to control. Based on this property, reversible dispersion and release of SWNTs in the solution phase were achieved, which are expected to find usefulness in making SWNT-based semiconducting electronic devices. In conclusion, our current work has demonstrated that DTF is a fascinating substituent group which not only introduces rich redox and electronic properties, but also can bring about novel chemical reactivities, photophysical and supramolecular properties to organic functional materials. Continued exploration of DTF as a versatile building block in various molecular and supramolecular systems is anticipated to produce fruitful results.

## Experimental

### Materials

Chemicals were purchased from commercial suppliers and used directly without purification. HiPCO SWNTs were purchased from Carbon Nanotechnologies Inc. CoMoCAT SWNTs were purchased from Southwest NanoTechnologies Inc. Thione 4,<sup>19</sup> compounds 6 (ref. 7c and 20) and 10 (ref. 7c and 20) were prepared according to the literature procedures.

### Synthesis

**4,4'-(1,4-Phenylenebis(ethyne-2,1-diyl))dibenzaldehyde (3).** To an oven-dried round-bottom flask protected under N<sub>2</sub> were charged *p*-ethynylbenzaldehyde (1) (0.354 g, 2.72 mmol),

1,4-diiodobenzene (2) (0.409 g, 1.23 mmol), PdCl<sub>2</sub>(PPh<sub>3</sub>)<sub>2</sub> (21.2 mg, 0.0299 mmol), CuI (11.5 mg, 0.0603 mmol), and Et<sub>3</sub>N (40 mL). The solution was degassed by N<sub>2</sub> bubbling at room temperature for 5 min, and then the resultant solution was heated to 45 °C under stirring and N<sub>2</sub> protection overnight. Solids precipitated out of the reaction mixture were collected by vacuum filtration, washed with CH<sub>2</sub>Cl<sub>2</sub> and air dried to give compound 3 (0.365 g, 1.09 mmol, 78% crude) as an off-white solid. M.p. 191–194 °C; IR (neat): 1696, 1595, 1417, and 1204 cm<sup>-1</sup>; meaningful <sup>1</sup>H NMR and <sup>13</sup>C spectra of 3 could not be obtained due to poor solubility. HRMS (MALDI-TOF, +eV) *m/z* calcd for C<sub>24</sub>H<sub>14</sub>O: 334.0994; found: 334.1039 [M]<sup>+</sup>.

**DTF-OPE 5.** A solution of thione 4 (0.109 g, 0.396 mmol) and compound 3 (0.342 g, 0.172 mmol) in trimethylphosphite (20 mL) was stirred and heated to 130 °C for about 6 h under a N<sub>2</sub> atmosphere, then the excess trimethylphosphite was removed by vacuum distillation, and the resulting crude product was purified by silica flash column chromatography (EtOAc-hexanes, 1:99) followed by recrystallization from acetone to yield pure compound 5 (0.0500 g, 0.0418 mmol, 13%) as a yellow solid. M.p. 103–104 °C; IR (neat): 2916, 2846, 1571, 1414, 933 cm<sup>-1</sup>; <sup>1</sup>H NMR (500 MHz, CD<sub>2</sub>Cl<sub>2</sub>)  $\delta$  = 7.52 (t, *J* = 5.2 Hz, 8H), 7.22 (d, *J* = 8.4 Hz, 4H), 6.49 (s, 2H), 2.85 (td, *J* = 7.3, 2.6 Hz, 8H), 1.69–1.62 (m, 8H), 1.45–1.39 (m, 8H), 1.32–1.27 (m, 48H), 0.89–0.86 ppm (m, 12H); <sup>13</sup>C NMR (75 MHz, CD<sub>2</sub>Cl<sub>2</sub>)  $\delta$  = 136.9, 134.9, 132.1, 131.9, 128.3, 126.9, 125.4, 123.5, 120.1, 113.6, 91.9, 89.9, 36.6, 36.5, 32.3, 30.3, 30.2, 29.97, 29.93, 29.7, 29.5, 28.92, 28.90, 23.0, 14.3 ppm; HRMS (MALDI-TOF, +eV) *m/z* calcd for C<sub>70</sub>H<sub>98</sub>S<sub>8</sub>: 1194.5434; found: 1194.5444 [M]<sup>+</sup>.

**Aldehyde-OPE 7.** To an oven-dried round-bottom flask protected under N<sub>2</sub> were charged compound 6 (0.102 g, 0.309 mmol), 1,4-diiodobenzene (2) (0.369 g, 0.679 mmol), PdCl<sub>2</sub>(PPh<sub>3</sub>)<sub>2</sub> (5.30 mg, 0.0075 mmol), CuI (2.80 mg, 0.014 mmol), and Et<sub>3</sub>N (50 mL). The solution was degassed by N<sub>2</sub> bubbling at room temperature for 5 min, and then the resultant solution was heated to 45 °C under stirring and N<sub>2</sub> protection overnight. After the reaction was complete as checked by TLC analysis, the solvent was removed by rotary evaporation. The residue was diluted with CH<sub>2</sub>Cl<sub>2</sub> and the diluted residue was filtered through a MgSO<sub>4</sub> pad. The solvent was removed by vacuum evaporation and the residue was washed with hexanes to give pure compound 7 (0.275 g, 0.237 mmol, 78%) as a yellow solid. M.p. 123–124 °C; IR (neat): 2919, 2850, 1698, 1596, 1459, 1212, 943 cm<sup>-1</sup>; <sup>1</sup>H NMR (300 MHz, CDCl<sub>3</sub>)  $\delta$  = 10.02 (s, 2H), 7.87 (d, *J* = 8.4 Hz, 4H), 7.68 (d, *J* = 8.2 Hz, 4H), 7.51 (s, 4H), 7.03 (d, *J* = 0.9 Hz, 4H), 4.05 (t, *J* = 6.4 Hz, 8H), 1.91–1.82 (m, 8H), 1.60–1.50 (m, 8H), 1.41–1.25 (m, 48H), 0.89–0.85 ppm (m, 12H); <sup>13</sup>C NMR (75 MHz, CDCl<sub>3</sub>)  $\delta$  = 191.3, 153.9, 153.7, 135.4, 132.0, 131.5, 129.8, 129.6, 123.3, 116.9, 116.8, 114.7, 113.3, 95.0, 94.0, 90.2, 87.9, 69.7, 69.6, 31.91, 31.90, 29.7, 29.6, 29.43, 29.36, 29.33, 26.1, 22.70, 22.68, 14.14, 14.12 ppm; HRMS (MALDI-TOF, +eV) *m/z* calcd for C<sub>80</sub>H<sub>102</sub>O<sub>6</sub>: 1158.7676; found: 1158.7665 [M]<sup>+</sup>.

**DTF-oligomer 8.** A solution of thione 4 (0.190 g, 0.396 mmol) and compound 7 (0.200 g, 0.172 mmol) in trimethylphosphite (15 mL) was stirred and heated to 130 °C for about 3 h under a N<sub>2</sub> atmosphere. On completion, the excess trimethylphosphite was removed by vacuum distillation. The obtained crude

product was purified by silica flash column chromatography (EtOAc–hexanes, 1 : 99) followed by recrystallization from acetone to yield pure compound **8** (0.264 g, 0.131 mmol, 76%) as a yellow solid. M.p. 81–82 °C; IR (neat): 2918, 2850, 1568, 1460, 1212, 1059 cm<sup>-1</sup>; <sup>1</sup>H NMR (500 MHz, CD<sub>2</sub>Cl<sub>2</sub>) δ = 7.52–7.50 (m, 8H), 7.22 (d, *J* = 8.6 Hz, 4H), 7.03 (s, 4H), 6.49 (s, 2H), 4.04 (td, *J* = 6.4, 1.9 Hz, 8H), 2.84 (td, *J* = 7.4, 1.8 Hz, 8H), 1.88–1.83 (m, 8H), 1.69–1.52 (m, 8H), 1.59–1.54 (m, 8H), 1.56–1.50 (m, 4H), 1.45–1.37 (m, 16H), 1.34–1.27 (m, 88H), 0.89–0.86 ppm (m, 24H); <sup>13</sup>C NMR (75 MHz, CDCl<sub>3</sub>) δ = 154.1, 154.0, 136.7, 134.7, 132.0, 131.8, 128.4, 126.9, 125.4, 123.7, 120.5, 117.2, 117.1, 114.7, 113.9, 113.7, 95.6, 94.8, 88.5, 87.0, 70.0, 32.3, 36.6, 36.5, 32.3, 30.3, 30.2, 30.1, 30.0, 29.97, 29.94, 29.84, 29.77, 29.73, 29.55, 29.53, 28.93, 28.91, 26.5, 23.11, 23.09, 14.31, 14.28 ppm; HRMS (MALDI-TOF, +eV) *m/z* calcd for C<sub>126</sub>H<sub>186</sub>O<sub>4</sub>S<sub>8</sub>: 2019.2117; found: 2019.2097 [M]<sup>+</sup>.

**1,4-Bis(*E*)-2-iodostyryl)benzene (**11**).** To an oven-dried flask protected under N<sub>2</sub> were charged bisphosphonate **10** (1.03 g, 2.64 mmol), NaH (0.320 g, 60%, 7.92 mmol), and dry THF (50 mL). The solution was observed to gradually turn into a dark yellow colour at 50 °C. A solution of *o*-iodobenzaldehyde (**9**) (1.21 g, 5.21 mmol) in THF (20 mL) was added in small portions over a period of 10 min *via* a syringe. The reaction was kept under stirring at the same temperature for another 30 min before workup. After the reaction was complete as checked by TLC analysis, the reaction mixture was poured into ice, and the resulting solid was extracted with CH<sub>2</sub>Cl<sub>2</sub> and the organic layer was washed with water several times and then dried over MgSO<sub>4</sub>, concentrated under vacuum to afford compound **11** which was finally washed with methanol to give to the pure form (0.690 g, 1.29 mmol, 49%) as a yellow solid. M.p. 159–161 °C; IR (neat): 1460, 1424, 1007, 957, 814 cm<sup>-1</sup>; <sup>1</sup>H NMR (500 MHz, CDCl<sub>3</sub>) δ = 7.89 (dd, *J* = 7.9, 1.1 Hz, 2H), δ 7.65 (dd, *J* = 7.8, 1.5 Hz, 2H), 7.57 (s, 4H), 7.37–7.34 (m, 4H), 7.00–6.95 ppm (m, 4H); <sup>13</sup>C NMR (75 MHz, CDCl<sub>3</sub>) δ = 140.2, 139.7, 136.7, 132.6, 131.1, 129.0, 128.4, 127.2, 126.2, 100.6 ppm; HRMS (EI-TOF, +eV) *m/z* calcd for C<sub>22</sub>H<sub>16</sub>I<sub>2</sub>: 533.9341; found 533.9336 [M]<sup>+</sup>.

**Aldehyde-OPV **12**.** To an oven-dried round-bottom flask protected under N<sub>2</sub> were charged compound **11** (0.301 g, 0.561 mmol), compound **1** (0.183 g, 1.40 mmol), PdCl<sub>2</sub>(PPh<sub>3</sub>)<sub>2</sub> (9.80 mg, 0.0139 mmol), CuI (5.30 mg, 0.027 mmol), and Et<sub>3</sub>N (50 mL). The solution was degassed by N<sub>2</sub> bubbling at room temperature for 5 min, and then the resultant solution was heated to 45 °C under stirring and N<sub>2</sub> protection overnight. After the reaction was complete as checked by TLC analysis, the solvent was removed by rotary evaporation. The residue was diluted with CH<sub>2</sub>Cl<sub>2</sub> and the diluted residue was filtered through a MgSO<sub>4</sub> pad. The solution obtained was washed with water, dried over MgSO<sub>4</sub>, and concentrated under vacuum to give crude product **12**, which was further purified by silica flash column chromatography (hexanes–EtOAc, 95 : 15) to yield pure compound **12** (0.197 g, 0.366 mmol, 65%) as a yellow solid. M.p. 175–178 °C; IR (neat): 1695, 1598, 1389, 1293, 1206, 1158, 1013 cm<sup>-1</sup>; <sup>1</sup>H NMR (500 MHz, CDCl<sub>3</sub>) δ = 10.04 (s, 2H), 7.91–7.87 (m, 4H), 7.76–7.70 (m, 8H), 7.59–7.58 (m, 4H), 7.40 (t, *J* = 7.4 Hz, 2H), 7.30–7.23 ppm (m, 2H); a meaningful <sup>13</sup>C NMR spectrum of **12** could not be obtained due to its limited solubility. HRMS

(MALDI-TOF, +eV) *m/z* calcd for C<sub>40</sub>H<sub>26</sub>O<sub>2</sub>: 538.1933; found: 538.1939 [M]<sup>+</sup>.

**DTF-oligomer **13**.** A solution of thione **4** (0.408 mg, 0.888 mmol) and compound **12** (0.208 g, 0.386 mmol) in trimethylphosphite (15 mL) was stirred and heated to 130 °C for about 3 h under a N<sub>2</sub> atmosphere, and then the excess trimethylphosphite was removed by vacuum distillation. The obtained crude product was purified by silica flash column chromatography (EtOAc–hexanes, 1 : 99) to yield pure compound **13** (0.362 g, 0.258 mmol, 67%) as thick syrup. IR (neat): 2919, 2849, 1671, 1599, 1458, 1259, 957 cm<sup>-1</sup>; <sup>1</sup>H NMR (500 MHz, CDCl<sub>3</sub>) δ = 7.77 (d, *J* = 16.4 Hz, 2H), 7.73 (d, *J* = 7.7 Hz, 2H), 7.60 (s, 4H), 7.56 (d, *J* = 7.7 Hz, 4H), 7.34 (t, *J* = 7.5 Hz, 2H), 7.25–7.20 (m, 6H), 6.45 (s, 2H), 2.84–2.79 (m, 8H), 1.69–1.60 (m, 8H), 1.42–1.37 (m, 8H), 1.29–1.24 (m, 48H), 0.89–80 ppm (m, 12H); <sup>13</sup>C NMR (75 MHz, CDCl<sub>3</sub>) δ = 138.9, 137.5, 136.9, 134.9, 132.9, 132.0, 130.1, 128.9, 128.3, 127.8, 127.5, 127.0, 125.4, 125.1, 122.7, 120.4, 113.6, 95.3, 88.9, 36.6, 36.5, 32.3, 30.3, 30.1, 29.9, 29.7, 29.6, 28.96, 28.91, 23.1, 18.9, 14.3 ppm; HRMS (MALDI-TOF, +eV) *m/z* calcd for C<sub>86</sub>H<sub>110</sub>S<sub>8</sub>: 1398.6373; found 1398.6267 [M]<sup>+</sup>.

**Aldehyde-oligomer **14**.** To an oven-dried round-bottom flask protected under N<sub>2</sub> were charged compound **11** (0.260 g, 0.490 mmol), compound **6** (0.661 g, 1.07 mmol), PdCl<sub>2</sub>(PPh<sub>3</sub>)<sub>2</sub> (6.80 mg, 0.0970 mmol), CuI (3.60 mg, 0.0194 mmol), and Et<sub>3</sub>N (100 mL). The solution was degassed by N<sub>2</sub> bubbling at room temperature for 5 min, and then the resultant solution was heated to 45 °C under stirring and N<sub>2</sub> protection overnight. After the reaction was complete as checked by TLC analysis, the solvent was removed by rotary evaporation. The residue was diluted with CH<sub>2</sub>Cl<sub>2</sub> and the diluted residue was filtered through a MgSO<sub>4</sub> pad. The solution obtained was washed with water, dried over MgSO<sub>4</sub>, and concentrated under vacuum to give crude product **14**, which was further purified by silica flash column chromatography (hexanes–EtOAc, 9 : 1) to yield pure compound **14** (0.480 g, 0.352 mmol, 72%) as a yellow solid. M.p. 153–155 °C; IR (neat): 2919, 2851, 2204, 1704, 1598, 1420, 1340, 1213 cm<sup>-1</sup>; <sup>1</sup>H NMR (500 MHz, CDCl<sub>3</sub>) δ = 10.00 (s, 2H), 7.84–7.81 (m, 8H), 7.74 (d, *J* = 7.9 Hz, 2H), 7.65 (d, *J* = 8.2 Hz, 4H), 7.58–7.56 (m, 4H), 7.35 (t, *J* = 7.7 Hz, 2H), 7.25–7.22 (m, 4H), 7.06 (s, 4H), 4.03 (t, *J* = 6.3 Hz, 8H), 1.87–1.81 (m, 4H), 1.76–1.71 (m, 4H), 1.56–1.46 (m, 8H), 1.41–1.31 (m, 12H), 1.27–1.16 (m, 36H), 0.86–0.82 ppm (m, 12H); <sup>13</sup>C NMR (75 MHz, CDCl<sub>3</sub>) δ = 191.3, 153.9, 153.6, 138.8, 137.1, 135.3, 132.7, 132.0, 129.8, 129.5, 128.6, 127.3, 127.2, 126.9, 124.7, 122.4, 117.2, 116.8, 115.2, 113.1, 93.98, 93.95, 91.1, 90.3, 77.2, 69.9, 69.6, 45.8, 31.89, 31.87, 29.7, 29.61, 29.59, 29.56, 29.5, 29.4, 29.2, 26.1, 25.9, 22.7, 14.1 ppm; HRMS (MALDI-TOF, +eV) *m/z* calcd for C<sub>96</sub>H<sub>114</sub>O<sub>6</sub>: 1362.8615; found: 1362.8542 [M]<sup>+</sup>.

**DTF-oligomer **15**.** A solution of thione **4** (0.169 g, 0.354 mmol) and compound **14** (0.210 g, 0.153 mmol) in trimethylphosphite (15 mL) was stirred and heated to 130 °C for about 3 h under a N<sub>2</sub> atmosphere, and then the excess trimethylphosphite was removed by vacuum distillation. The obtained crude product was purified by silica flash column chromatography (EtOAc–hexanes, 1 : 99) followed by recrystallization from acetone to yield pure compound **15** (0.240 g, 0.107 mmol, 71%) as a yellow solid. M.p. 92–93 °C; IR (neat): 2918, 2948,

1601, 1565, 1419, 1383, 1213, 1027  $\text{cm}^{-1}$ ;  $^1\text{H}$  NMR (500 MHz,  $\text{CD}_2\text{Cl}_2$ )  $\delta$  = 7.85 (d,  $J$  = 16.4 Hz, 2H), 7.77 (d,  $J$  = 7.9 Hz, 2H), 7.61 (s, 4H), 7.57 (dd,  $J$  = 7.7, 1.0 Hz, 2H), 7.49 (d,  $J$  = 8.4 Hz, 4H), 7.37 (td,  $J$  = 7.5, 1.0 Hz, 2H), 7.29–7.25 (m, 4H), 7.18 (d,  $J$  = 8.4, 4H), 7.07 (d,  $J$  = 0.8 Hz, 4H), 6.46 (s, 2H), 4.04 (td,  $J$  = 6.7, 3.1 Hz, 8H), 2.84 (td,  $J$  = 6.6, 0.9 Hz, 8H), 1.86–1.81 (m, 4H), 1.77–1.71 (m, 4H), 1.69–1.62 (m, 8H), 1.56–1.50 (m, 4H), 1.45–1.35 (m, 16H), 1.34–1.17 (m, 92H), 0.90–0.82 ppm (m, 24H);  $^{13}\text{C}$  NMR (75 MHz,  $\text{CD}_2\text{Cl}_2$ )  $\delta$  = 154.0, 139.1, 137.5, 136.7, 134.6, 132.9, 132.0, 130.2, 129.0, 128.4, 127.7, 127.6, 127.2, 126.9, 125.3, 125.1, 122.8, 120.6, 117.2, 114.6, 114.3, 113.7, 95.6, 93.7, 91.8, 87.1, 70.2, 70.1, 36.6, 36.5, 32.32, 32.29, 30.3, 30.2, 30.1, 30.0, 29.98, 29.94, 29.89, 29.82, 29.79, 29.76, 29.74, 29.6, 29.56, 29.54, 28.94, 28.92, 26.6, 26.4, 23.12, 23.09, 14.32, 14.29 ppm; HRMS (MALDI-TOF, +eV)  $m/z$  calcd for  $\text{C}_{142}\text{H}_{198}\text{O}_4\text{S}_8$ : 2223.3056; found 2223.3082  $[\text{M}]^+$ .

**Synthesis of 14 by fullerene-sensitized oxidation of 15.** To a solution of compound 15 (10.3 mg, 0.00462 mmol) in benzene (1 mL) was added  $\text{C}_{60}$  fullerene (10.1 mg, 0.0140 mmol). The reaction mixture was stirred at room temperature for 20 h in the presence of air. The reaction mixture was then diluted and extracted with ethylacetate. The organic layer was washed with water, dried over  $\text{MgSO}_4$ , and concentrated under vacuum to give crude 14. Pure compound 14 (5.60 mg, 0.00410 mmol, 89%) was obtained after silica column chromatographic separation (hexanes–EtOAc, 9 : 1) and its molecular structure was confirmed by  $^1\text{H}$ ,  $^{13}\text{C}$  NMR, and MALDI-TOF MS analyses.

## Apparatus

All reactions were conducted in standard, dry glassware and under an inert atmosphere of nitrogen unless otherwise noted. Evaporation and concentration were carried out with a water-aspirator. Flash column chromatography was performed using 240–400 mesh silica gel, and thin-layer chromatography (TLC) was carried out with silica gel F254 covered on plastic sheets and visualized by UV light. Melting points (m.p.) were measured with the SRS OptiMelt melting point apparatus and are uncorrected.  $^1\text{H}$  and  $^{13}\text{C}$  NMR spectra were recorded on a Bruker Avance 500 MHz spectrometer and a Bruker Avance III 300 MHz multinuclear spectrometer. Chemical shifts ( $\delta$ ) are reported in ppm downfield from the signal of the internal reference  $\text{SiMe}_4$  for  $^1\text{H}$  and  $^{13}\text{C}$  NMR spectra. Coupling constants ( $J$ ) are given in Hz. Infrared spectra (IR) were recorded on a Bruker tensor 27 spectrometer. UV-Vis-NIR absorption spectra were recorded on a Cary 6000i spectrophotometer. Emission spectra were recorded on a Photon Technology International (PTI) Quanta-master 6000 spectrofluorometer equipped with a continuous xenon arc lamp as the excitation source. Atomic force microscopy (AFM) images were taken with a Q-Scope AFM operated in the tapping mode. Raman spectra were recorded on a Horiba Jobin Yvon confocal Raman spectrometer operated at a laser wavelength of 534 nm. Cyclic voltammetric (CV) experiments were carried out in a standard three-electrode setup controlled by a BASi Epsilon workstation. MALDI-TOF MS analyses were performed on an Applied Biosystems Voyager instrument using dithranol as the matrix.

## Acknowledgements

The authors thank Natural Sciences and Engineering Research Council of Canada (NSERC) and Canada Foundation for Innovation (CFI) for funding support.

## Notes and references

- (a) D. Lorcy, R. Carlier, A. Robert, A. Tallec, P. Le Magueres and L. Ouahab, *J. Org. Chem.*, 1995, **60**, 2443–2447; (b) J. Roncali, *J. Mater. Chem.*, 1997, **7**, 2307–2321; (c) N. Bellec, K. Boubekeur, R. Carlier, P. Hapiot, D. Lorcy and A. Tallec, *J. Phys. Chem. A*, 2000, **104**, 9750–9759; (d) R. Carlier, P. Hapiot, D. Lorcy, A. Robert and A. Tallec, *Electrochim. Acta*, 2001, **46**, 3269–3277; (e) J. Massue, N. Bellec, M. Guerro, J.-F. Bergamini, P. Hapiot and D. Lorcy, *J. Org. Chem.*, 2007, **72**, 4655–4662; (f) Y. Zhao, G. Chen, K. Mulla, I. Mahmud, S. Liang, P. Dongare, D. W. Thompson, L. N. Dawe and S. Bouzan, *Pure Appl. Chem.*, 2012, **84**, 1005–1025.
- (a) D. Lorcy, J. Rault-Berthelot and C. Poriel, *Electrochem. Commun.*, 2000, **2**, 382–385; (b) K. Naka, S. Inagi and Y. Chujo, *J. Polym. Sci., Part A: Polym. Chem.*, 2005, **43**, 4600–4608; (c) K. Naka, S. Inagi, Y. Murachi and Y. Chujo, *J. Polym. Sci., Part A: Polym. Chem.*, 2006, **44**, 2027–2033; (d) P. Frère and P. J. Skabara, *Chem. Soc. Rev.*, 2005, **34**, 69–98; (e) T. Uemura, K. Naka and Y. Chujo, in *New Synthetic Methods*, Springer, Berlin, 2004, vol. 167, pp. 81–106.
- (a) N. Cocherel, P. Leriche, E. Ripaud, N. Gallego-Planas, P. Frere and J. Roncali, *New J. Chem.*, 2009, **33**, 801–806; (b) E. Ripaud, P. Leriche, N. Cocherel, T. Cauchy, P. Frere and J. Roncali, *Org. Biomol. Chem.*, 2011, **9**, 1034–1040.
- S. Alías, R. Andreu, M. J. Blesa, M. A. Cerdán, S. Franco, J. Garín, C. López, J. Orduna, J. Sanz, R. Alicante, B. Villacampa and M. Allain, *J. Org. Chem.*, 2008, **73**, 5890–5898.
- K. Guo, K. Yan, X. Lu, Y. Qiu, Z. Liu, J. Sun, F. Yan, W. Guo and S. Yang, *Org. Lett.*, 2012, **14**, 2214–2217.
- (a) G. Chen, I. Mahmud, L. N. Dawe, D. Lee and Y. Zhao, *J. Org. Chem.*, 2011, **76**, 2701–2715; (b) G. Chen, I. Mahmud, L. Dawe and Y. Zhao, *Org. Lett.*, 2010, **12**, 704–707.
- (a) A. J. Zuccherro, P. L. McGrier and U. H. F. Bunz, *Acc. Chem. Res.*, 2009, **43**, 397–408; (b) N. Zhou, L. Wang, D. W. Thompson and Y. Zhao, *Org. Lett.*, 2008, **10**, 3001–3004; (c) N. Zhou, L. Wang, D. W. Thompson and Y. Zhao, *Tetrahedron*, 2011, **67**, 125–143.
- C. A. Christensen, A. S. Batsanov and M. R. Bryce, *J. Org. Chem.*, 2007, **72**, 1301–1308.
- H. Wang, J. Mei, P. Liu, K. Schmidt, G. Jiménez-Osés, S. Osuna, L. Fang, C. J. Tassone, A. P. Zoombelt, A. N. Sokolov, K. N. Houk, M. F. Toney and Z. Bao, *ACS Nano*, 2013, **7**, 2659–2668.
- (a) P. Blanchard, M. Sallé, G. Duguay, M. Jubault and A. Gorgues, *Tetrahedron Lett.*, 1992, **33**, 2685–2688; (b) R. P. Parg, J. D. Kilburn and T. G. Ryan, *Synthesis*, 1994, 195–198; (c) N. Svenstrup and J. Becher, *Synthesis*, 1995, 215–235.

- 11 (a) F. Langa and J.-F. Nierengarten, *Fullerenes: Principles and Applications*, Royal Society of Chemistry, Cambridge, 2007; (b) A. Hirsch and M. Brettreich, *Fullerenes: Chemistry and Reactions*, Wiley-VCH, Weinheim, 2005.
- 12 (a) H. Tokuyama and E. Nakamura, *J. Org. Chem.*, 1994, **59**, 1135–1138; (b) N. Chronakis, G. C. Vougioukalakis and M. Orfanopoulos, *Org. Lett.*, 2002, **4**, 945–948.
- 13 (a) L. F. M. L. Ciscato, D. Weiss, R. Beckert, E. L. Bastos, F. H. Bartoloni and W. J. Baader, *New J. Chem.*, 2011, **35**, 773–775; (b) N. Hoffmann, *Chem. Rev.*, 2008, **108**, 1052–1103; (c) W. Adam and W. J. Baader, *Angew. Chem., Int. Ed. Engl.*, 1984, **23**, 166–167.
- 14 (a) N. Karousis, N. Tagmatarchis and D. Tasis, *Chem. Rev.*, 2010, **110**, 5366–5397; (b) Y.-L. Zhao and J. F. Stoddart, *Acc. Chem. Res.*, 2009, **42**, 1161–1171; (c) C. Backes and A. Hirsch, in *Chemistry of Nanocarbons*, John Wiley & Sons, Ltd, 2010, pp. 1–48; (d) C. Backes, *Noncovalent Functionalization of Carbon Nanotubes: Fundamental Aspects of Dispersion and Separation in Water*, Springer, Heidelberg, 2012; (e) B. P. Grady, *Macromol. Rapid Commun.*, 2010, **31**, 247–257.
- 15 (a) S. Liang, G. Chen, J. Peddle and Y. Zhao, *Chem. Commun.*, 2012, **48**, 3100–3102; (b) C. Romero-Nieto, R. García, M. Á. Herranz, C. Ehli, M. Ruppert, A. Hirsch, D. M. Guldi and N. Martín, *J. Am. Chem. Soc.*, 2012, **134**, 9183–9192; (c) A. Wurl, S. Goossen, D. Canevet, M. Sallé, E. M. Pérez, N. Martín and C. Klinke, *J. Phys. Chem. C*, 2012, **116**, 20062–20066; (d) E. M. Perez, B. M. Illescas, M. A. Herranz and N. Martín, *New J. Chem.*, 2009, **33**, 228–234; (e) C. Ehli, D. M. Guldi, M. Angeles Herranz, N. Martín, S. Campidelli and M. Prato, *J. Mater. Chem.*, 2008, **18**, 1498–1503.
- 16 (a) A. Jorio, G. Dresselhaus and M. S. Dresselhaus, *Carbon Nanotubes: Advanced Topics in the Synthesis, Structure, Properties and Application*, Springer, Berlin, 2008; (b) S. Reich, C. Thomsen and J. Maultzsch, *Carbon Nanotubes: Basic Concepts and Physical Properties*, Wiley-VCH, Weinheim, 2004; (c) M. Meyyappan, *Carbon Nanotubes: Science and Applications*, CRC Press, Boca Raton, 2004.
- 17 For recent reports on reversible dispersion and release of SWNTs, see: (a) Z. Zhang, Y. Che, R. A. Smaldone, M. Xu, B. R. Bunes, J. S. Moore and L. Zang, *J. Am. Chem. Soc.*, 2010, **132**, 14113–14117; (b) D. Wang and L. Chen, *Nano Lett.*, 2007, **7**, 1480–1484; (c) S. Chen, Y. Jiang, Z. Wang, X. Zhang, L. Dai and M. Smet, *Langmuir*, 2008, **24**, 9233–9236; (d) P. Imin, M. Imit and A. Adronov, *Macromolecules*, 2012, **45**, 5045–5050; (e) Y. Ding, S. Chen, H. Xu, Z. Wang, X. Zhang, T. H. Ngo and M. Smet, *Langmuir*, 2010, **26**, 16667–16671; (f) G. Yu, M. Xue, Z. Zhang, J. Li, C. Han and F. Huang, *J. Am. Chem. Soc.*, 2012, **134**, 13248–13251; (g) S. Liang, G. Chen, J. Peddle and Y. Zhao, *Chem. Commun.*, 2012, **48**, 3100–3102.
- 18 A. M. Fracaroli, A. M. Granados and R. H. de Rossi, *J. Org. Chem.*, 2009, **74**, 2114–2119.
- 19 (a) A. J. Moore and M. R. Bryce, *Tetrahedron Lett.*, 1992, **33**, 1373–1376; (b) G. Chen and Y. Zhao, *Tetrahedron Lett.*, 2006, **47**, 5069–5073.
- 20 Y. Zhao, Y. Shirai, A. D. Slepko, L. Cheng, L. B. Alemany, T. Sasaki, F. A. Hegmann and J. M. Tour, *Chem.-Eur. J.*, 2005, **11**, 3643–3658.